Reprinted from the Journal of the American Ceramic Society, Vol. 69, No. 3, March 1986

Structure of Incoherent ZrO_2/Al_2O_3 Interfaces

S. P. KRAUS-LANTERI,* T. E. MITCHELL,* and A. H. HEUER*

Department of Metallurgy and Materials Science, Case Western Reserve University, Cleveland, Ohio 44106

High-resolution electron microscopy was used to image incoherent ZrO_2/Al_2O_3 interfaces in ZrO_2-toughened Al_2O_3 containing intragranular ZrO_2. These particles are generally spherical but are sometimes faceted. High-resolution electron micrographs provide atomic-level information on the interfacial structure. For spherical particles, both ledgelike images and misfit dislocation-like images accommodated the lattice misfit, depending on the orientation of the interface, while faceted particles imply at least one low-energy ZrO_2/Al_2O_3 interface.

I. Introduction

ZIRCONIA-TOUGHENED alumina (ZTA) is the most important member of the wide class of ZrO_2-containing dispersion-toughened ceramics.[1] Such materials typically consist of modest amounts of ZrO_2 (up to 30 vol%) dispersed in a fine-grained Al_2O_3 matrix. The ZrO_2 particles can have tetragonal (t) or monoclinic (m) symmetry, are incoherent with the Al_2O_3 matrix, and can be either intergranular or intragranular (Fig. 1).

In the present paper, we will show high-resolution electron micrographs which provide information on the nature of the incoherent ZrO_2/Al_2O_3 interfaces on an atomic level, particularly for intragranular ZrO_2 particles. Intergranular ZrO_2/Al_2O_3 interfaces appear to be wetted by an amorphous grain-boundary phase;[2] these interfaces have also been imaged by high-resolution electron microscopy (HREM), but these results will be reported elsewhere.[3]

II. Experimental Procedure

ZTA samples containing 3.8, 10, and 15 vol% ZrO_2 have been studied using HREM; the fabrication or provenance of the samples is described elsewhere.[2] All microscopy was performed in a transmission electron microscope* dedicated to HREM and fitted with a top entry $\pm 10°$ tilting stage; the TEM pole piece has a C_s (spherical aberration constant) of 1.1 mm. This microscope routinely provides point-to-point resolution down to 0.236 nm.

Thin-foil HREM samples were prepared by ion beam thinning using conventional means, except that the thinned foils were annealed at 1200°C for 15 min before HREM examination. This annealing induced the (reverse) $m \rightarrow t$ transformation in particles in which the (forward) $t \rightarrow m$ transformation had occurred during foil preparation, a common occurrence in ZTA. (A preliminary report showing micrographs of an m-ZrO_2/Al_2O_3 interface, in which such a $t \rightarrow m$ transformation had occurred in an intragranular ZrO_2 particle during thin-foil preparation, has beeen published elsewhere.[4])

Before describing our results, we note that imaging conditions for HREM are very stringent. Firstly, the foil must be very thin, $\leq$20 to 30 nm. Secondly, both the ZrO_2 particle and the Al_2O_3 matrix have to be oriented such that a low index zone axis for both phases is exactly (or nearly) parallel to the electron beam. Because the ZrO_2 particles in these dispersion-toughened ceramics are randomly oriented with respect to their Al_2O_3 matrices, this requirement is very difficult to satisfy, particularly as the interface itself should also be parallel to the electron beam. Of the more than 100 ZrO_2 particles examined to date, only a handful satisfied these difficult constraints. In this paper, we report images of two intragranular ZrO_2/Al_2O_3 interfaces from which useful structural information can be obtained.

Thirdly, it is customary to take a through-focus series of images at various amounts of defocus, as the optimum defocus to achieve maximum structural information in the final image (the so-called Scherzer defocus) is difficult to know *a priori*.[5] Finally, unambiguous image interpretation requires exact image matching between computed (simulated) and experimental images, starting with assumed structural models and known microscope parameters (amount of defocus, C_s, etc.). While acceptable image matching for defect-free ZrO_2 or Al_2O_3 is straightforward (we have used both Skarnulis' CELLS program[6] and O'Keefe's SHRLI program[7] for this), modeling of the interface is much more difficult; this topic is currently a subject of much attention in our group. Because of the lack of computed interface images, our conclusions about interface structure must be considered tentative at this time.

III. Results and Discussion

Two ZrO_2 intragranular particles, one nearly spherical and one faceted, that satisfied the stringent HREM requirements are shown in Figs. 2(*A*) and (*B*), respectively. We discuss the spherical particle first.

Received August 2, 1985; approved September 3, 1985.
*Member, the American Ceramic Society.
*Model 200CX, JEOL USA Inc., Peabody, MA.

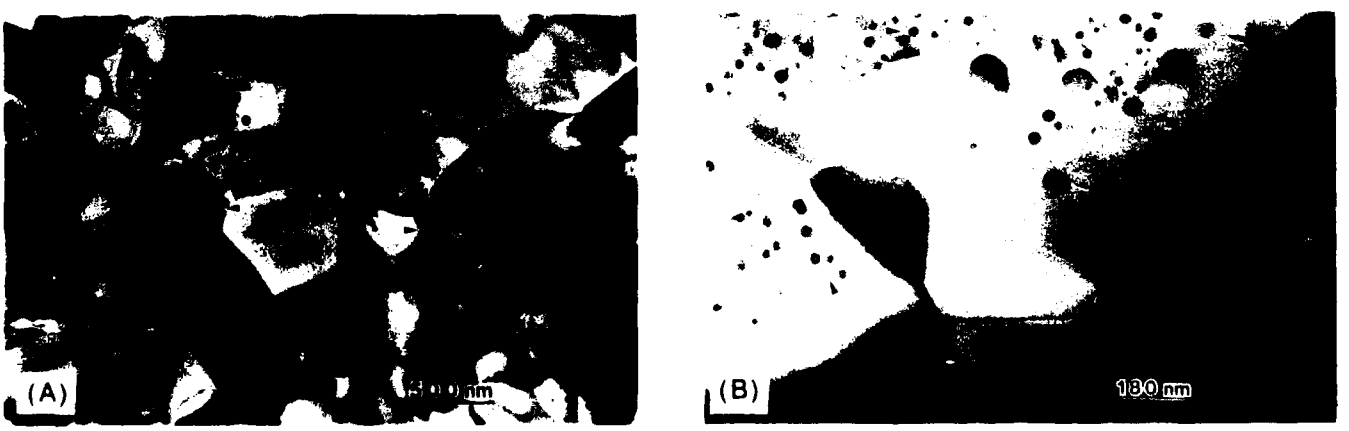

Fig. 1. Typical microstructure of ZrO_2-toughened Al_2O_3 showing (*A*) *inter*granular and (*B*) *intra*granular ZrO_2 particles; a few particles are arrowed.

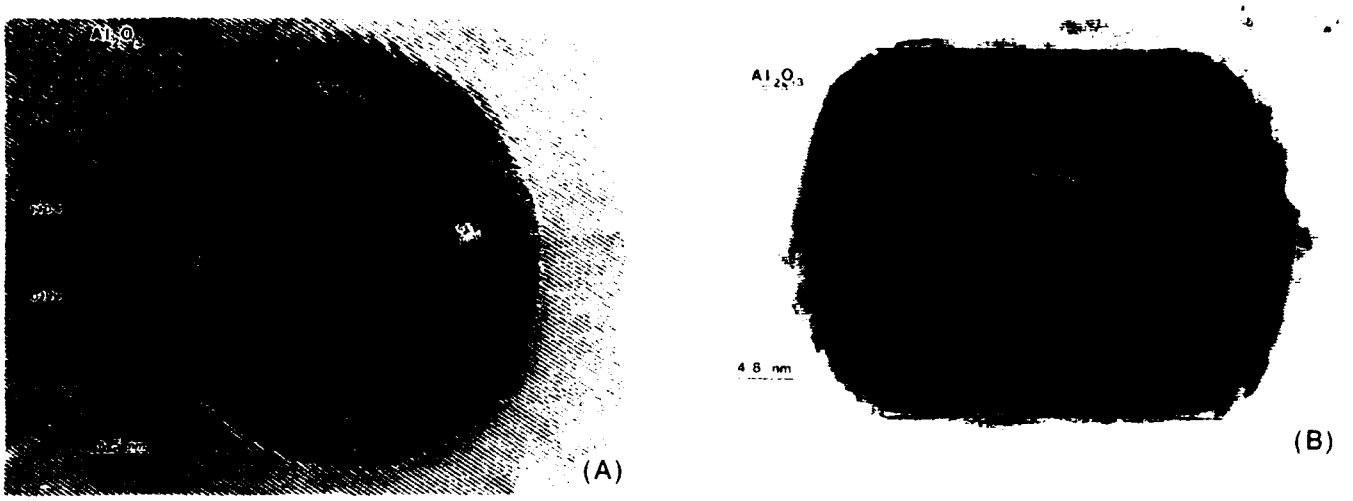

Fig. 2. (*A*) Intragranular ZrO_2 particle; a single set of (111) planes is visible in ZrO_2, while Al_2O_3 matrix is exactly oriented to $[3\bar{1}\,2\bar{1}]$ zone. (*B*) Faceted ZrO_2 particle in Al_2O_3 matrix, which is oriented exactly to $[10\bar{1}0]$ zone; note Moire fringes in ZrO_2 particle.

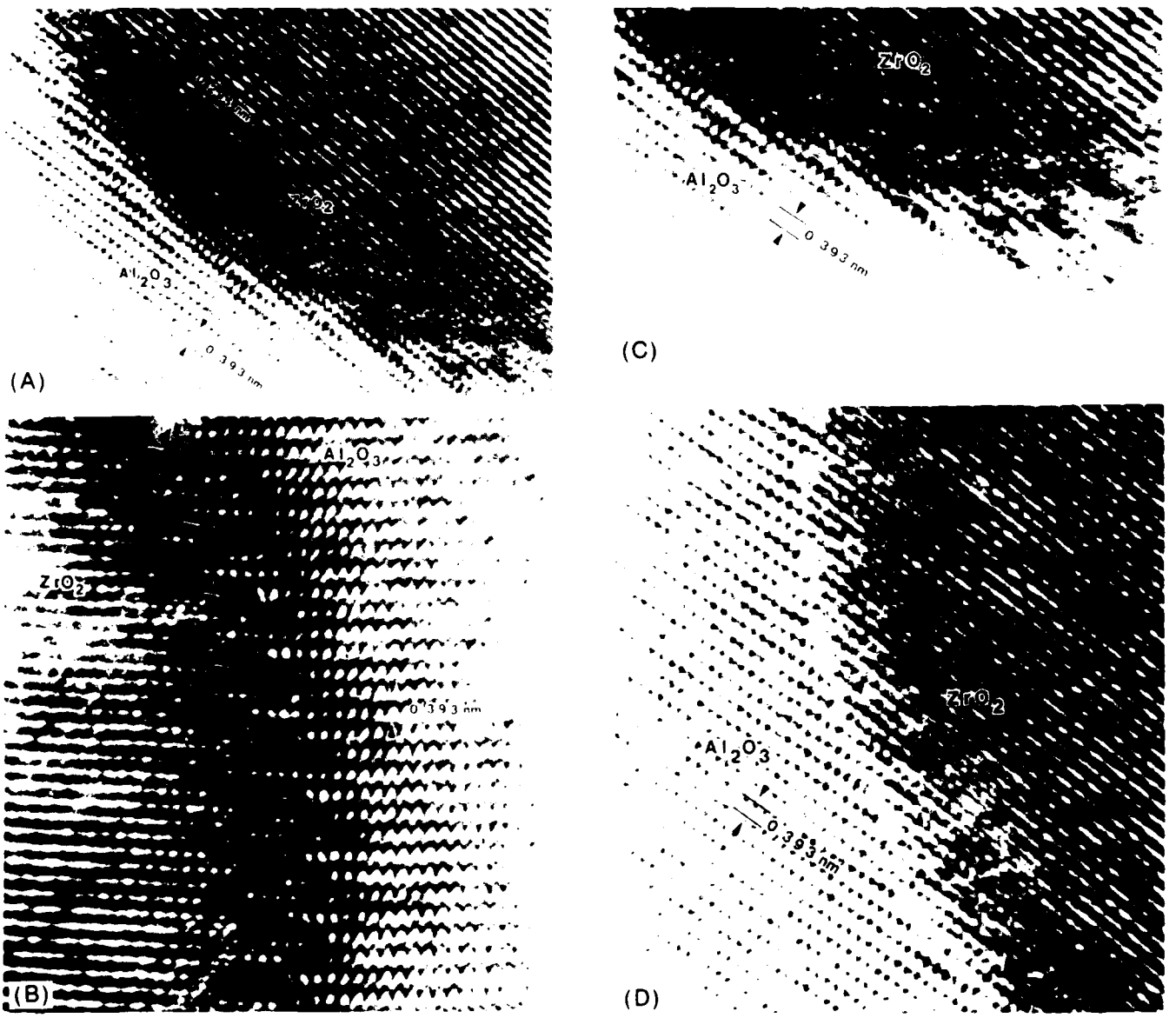

Fig. 3. Higher magnifications of various areas of Fig. 2(*A*). (*A*) Lattice mismatch accommodated by a series of ledges. (*B*) Periodicity changes along interface from every fourth Al_2O_3 plane stopping short of interface (arrowed) to every third one. (*C*) Lattice mismatch accommodated by misfit dislocations. (*D*) Interface which appears smooth; sighting along atomic planes reveals misfit dislocations.

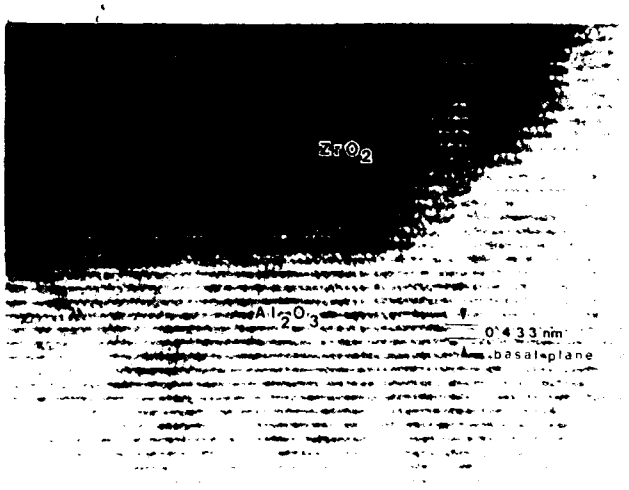

Fig. 4. Higher magnification of Fig. 2(*B*); Al_2O_3 basal plane (*d* spacing of 0.433 nm) is parallel to ZrO_2 facet.

As seen in the low-magnification micrograph of Fig. 2(*A*), the Al_2O_3 matrix is oriented exactly to the $[3\bar{1}\,\bar{2}1]$ zone axis and $(0\bar{1}11)$ and $(1\bar{1}0\bar{4})$ planes can be discerned. On the other hand, the ZrO_2 particle, which has *t* symmetry, has only a single set of (111) planes visible, as the closest zone axis ([110]) is tilted by a few degrees to the electron beam. The (111) ZrO_2 planes are misoriented by ≈5° from the $(0\bar{1}11)$ Al_2O_3 planes; furthermore, the *d* spacings for these two sets of planes differ significantly, 0.295 nm for (111) ZrO_2 and 0.393 nm for $(0\bar{1}11)$ Al_2O_3. In spite of this marked lattice mismatch, no microcracks or other gross distortions appear in the HREM image of the interface.

Various regions of the ZrO_2/Al_2O_3 interface are shown at higher magnification in Fig. 3. In the region shown in Fig. 3(*A*), the lattice mismatch between the two phases appears to be accommodated by a series of ledges, each one atomic plane high; such ledges are commonplace in semicoherent interfaces, as can occur between a precipitate and its matrix, but it is somewhat surprising to see them in the incoherent interface in Fig. 3(*A*).

Al_2O_3 and *t*-ZrO_2 have significantly different thermal expansion coefficients (7×10^{-6} to 8×10^{-6} and 9×10^{-6} to 11×10^{-6} °C^{-1}, respectively, depending on orientation), and thermoelastic strains between 0.2% and 0.4% are expected, assuming the system was stress free during sintering and stress relief mechanisms are inoperable below ≈1000°C. (Thermal strains of this order have been detected by Rühle and Kriven[5] using HVEM techniques.)

Evidence for such strain is also available in the image of Fig. 3(*A*). As noted above, the *t*-ZrO_2 is tilted ≈2° off its [110] zone axis such that only one set of (111) planes is being imaged. Near the interface, however, one set of (222) planes, with half the spacing of the (111) set, is visible, as well as an apparent structure image. We believe that the lattice bending due to these thermal expansion mismatch strains has tilted the lattice toward the [110] zone axis so that the (222) planes are apparent, but computer simulation is necessary to confirm this interpretation.

Figure 3(*B*) shows another region of the ZrO_2/Al_2O_3 interface, which accommodates the lattice mismatch without any apparent use of ledges. This region of the interface exhibits a type of periodic quasi-fringe contrast in the low-magnification image of Fig. 2(*A*). At higher magnification this periodic contrast (at the top of Fig. 3(*B*)) is seen to be due to every fourth Al_2O_3 plane (arrowed) extending less far into the interface than its neighboring planes. As the interface orientation changes, so does the period of the interface structure, so that near the center of Fig. 3(*B*), it is every third Al_2O_3 plane which stops short of the interface.

This periodic contrast has some similarities to misfit dislocations which can also exist in semicoherent interfaces to accommodate lattice mismatch; this type of mismatch accommodation is certainly in evidence in the region of interface shown in Fig. 3(*C*), although there are also ledgelike regions in conjunction with the dislocation-like regions in this micrograph. Finally, Fig. 3(*D*) shows a region of the interface which is apparently smooth and free of ledges; however, viewing along the planes of the images reveals the presence of periodic misfit dislocations. It appears that for this incoherent ZrO_2/Al_2O_3 interface, the lattice mismatch is accommodated by a combination of ledges and misfit dislocations, depending on interface orientation.

A higher-magnification image of the *faceted* interface of Fig. 2(*B*) is shown in Fig. 4. As noted in this figure, the facet plane is parallel to the basal plane of Al_2O_3 and this orientation of ZrO_2/Al_2O_3 interface must have a lower interfacial energy than any of the interface orientations of Fig. 3. Unfortunately, as will now be discussed, we have been unable so far to specify the ZrO_2 orientation that leads to this low-energy interface.

It is common in HREM to determine the crystal orientation of the material under study by taking an optical diffraction pattern of the image, using a laser diffractometer; and the crystal orientations shown in Fig. 3 were determined in this way. The Moiré fringes visible in Fig. 4 indicate that this is not possible with this image; in spite of the fact that this region of foil appeared to be quite thin (≈20 nm), the ZrO_2 particle apparently does not go through the foil and must be overlaid with some of the Al_2O_3 matrix. In fact, this suggests the existence of still another low-energy faceted ZrO_2/Al_2O_3 interface, in this case parallel to the $(10\bar{1}0)$ foil plane of Fig. 4. We are presently seeking other examples of faceted ZrO_2/Al_2O_3 interfaces in which the ZrO_2 extends through both the top and bottom of the foil so that the interface orientation can be specified exactly.

IV. Conclusion

HREM can be used to image incoherent ZrO_2/Al_2O_3 interfaces in ZTA. Both spherical and faceted ZrO_2 particles occur in ZTA; in the spherical particles, the mechanism of lattice accommodation of the two phases is a combination of ledges and misfit dislocations which depends on interface orientation.

The occurrence of faceted particles implies the existence of low-energy ZrO_2/Al_2O_3 interfaces. Although we are not yet able to specify the ZrO_2 orientation that leads to the low-energy interfaces, both basal (0001) and prism plane $\{11\bar{2}0\}$ Al_2O_3 orientations appear to be present.

References

[1]Advances in Ceramics, Vol. 12, Science and Technology of Zirconia II. Edited by N. Claussen, M. Rühle, and A. H. Heuer. American Ceramic Society, Columbus OH, 1984.
[2]B. Kibbel and A. H. Heuer, "Exaggerated Grain Growth in ZrO_2-Toughened Al_2O_3," this issue, pp. 231–36.
[3]S. P. Kraus-Lanteri; unpublished work.
[4]A. H. Heuer, S. Kraus-Lanteri, P. A. Labun, V. Lanteri, and T. E. Mitchell, "HREM Studies of Coherent and Incoherent Interfaces in ZrO_2-Containing Ceramics: A Preliminary Account", to be published in *Ultramicroscopy*.
[5]J. C. H. Spence, Experimental High-Resolution Electron Microscopy. Oxford University Press, New York, 1981.
[6]J. Skarnulis, "A System for Interactive Electron Image Calculations," *J. Appl. Crystallogr.*, **12**, 636–38 (1979).
[7]M. A. O'Keefe and P. R. Buseck, "Computation of High Resolution TEM Images of Minerals," *Trans. Am. Crystallogr. Assoc.*, **15**, 27–46 (1979).
[8]M. Rühle and W. M. Kriven, "Analysis of Strain Around Tetragonal and Monoclinic Zirconia Inclusions", Proceedings of an International Conference on Solid-Solid Phase Transformations. Edited by H. I. Aaronson, D. E. Laughlin, R. F. Sekerka, and C. M. Wayman. American Institute of Mining, Metallurgical and Petroleum Engineers, Pittsburgh, PA, 1982.